Density-dependent habitat selection alters fitness in a clonal hexapod

A thesis presented to

The Faculty of Graduate Studies

of

Lakehead University

by

KERMAN BAJINA

In partial fulfillment of requirements

for the degree of

Master of Science in Biology

April 11th 2019

Abstract

Density-dependent habitat selection shapes the distribution and abundance of organisms and thus informs our understanding of the eco-evolutionary process. When habitat choice is contingent on an individual's expectation of fitness, and when organisms are free to occupy the habitat they choose, their occupation of habitat is well described by an ideal free distribution (IFD). But when individuals are related, habitat selection that maximizes inclusive fitness (MAXN) allows cooperative individuals to supplant the IFD. I tested this possibility by measuring the fitness accrued through habitat selection by clonal populations of a common soil hexapod, *Folsomia candida*. I controlled variation associated with genetics and state-dependence by establishing experimental populations from a single founding mother and growing them under identical conditions. I varied habitat quality by manipulating substrate moisture. I allowed *F. candida* to choose between habitats and differentiated between IFD and MAXN habitat selection by measuring fitness. Surprisingly, habitat-selecting *F. candida* alter the expectations of fitness and can thus outcompete otherwise theoretically optimal strategies. My research demonstrates that density-dependent habitat selection is both an ultimate and proximate mechanism driving spatial population dynamics.

Lay Summary

Faculty and students in the Department of Biology are bound together by a common interest in explaining the diversity of life, the fit between form and function, and the distribution and abundance of organisms. Ecology, the science that studies distribution and abundance, is best done by developing theories and testing them with controlled experiments. An effective protocol is to imagine that adaptive evolution favours some strategies of habitat choice over others. The best strategy is one that yields the greatest benefit (fitness). Fitness of any single strategy of habitat choice depends on habitat quality, population density, and the frequency of alternative strategies. I tested these ideas using clonal populations of a common soil hexapod (springtails) in environments where I controlled habitat quality, identified habitat use, and measured the fitness of animals within each habitat. My experiments demonstrate that these springtails are "ideal" habitat selectors that appear to beat strategies posed by theory. These animals select habitat in a manner that changes the fitness they would achieve if otherwise deprived of choice. This profound result demonstrates the importance of controlled experiments on diminutive and "simple" organisms that provide new and challenging insights into the feedback between ecology and evolution.

Acknowledgements

Table of Contents

List of Tables

List of Figures

Introduction

A thorough understanding of mechanisms underlying the spatial dynamics of populations is necessary to fully comprehend the feedback between ecology and evolution and the conservation of biodiversity (Holt 1987, Tregenza 1995, Morris 2003a, Morris and Lundberg 2011). Spatial regulation occurs through the interaction between negative density-dependence within habitats (Rosenzweig 1981) and dispersal among them (Holt 1985, Morris 1988, Rodenhouse et al. 1997, Morris et al. 2004, Moses et al. 2013). If organisms are ideal habitat selectors, the isodar, the set of densities among habitats that equalizes expected fitness (Morris 1988), uniquely reveals all alternative forms of spatial regulation. Isodars also help explore temporal regulation within source-sink systems (Morris 2011a) and interactions among coexisting species (Morris 1988, Morris et al. 2000, Morris 2003b). Quantitative and qualitative differences in habitat, which generate each habitat's relationship with fitness (Morris 1988, Morris 1989, Morris 2011b), dictate the forms of spatial regulation (Morris 1988).

Optimal habitat selectors will disperse to match patterns in density with expectations of habitat differences in fitness (Morris and Davidson 2000). If unrelated individuals are unconstrained in their occupation of habitat, then they will obey an ideal-free distribution (IFD) in which habitat selection equalizes mean fitness among habitats (Fretwell and Lucas 1969). Evolutionary interests are contingent on the degree of relatedness (Hamilton 1963, Gardner and Welch 2011). So it is reasonable to ask: does the apparently evolutionarily stable strategy (ESS, Maynard Smith 1982) of the IFD resist invasion from an alternative strategy when individuals are related? The answer depends

on the inclusive fitness achieved by altruistic individuals that sacrifice occupation of a good habitat in favour of a poor one (so-called MAXN habitat selection, Morris 2011a).

I answer the question with controlled experiments. I begin with a brief assessment of IFD and MAXN strategies and how they can be differentiated. I then predict the expected outcomes of density-dependent habitat selection on populations of a clonal hexapod (*Folsomia candida*). I describe how I estimated fitness in different habitats across a range of population sizes, and how I merged those estimates with replicated experiments to test the theory. I evaluate the fit between data, theory, and the life-history of *F. candida*, and thus clarify the role of genetic relatedness on strategies of habitat selection. I conclude by documenting the crucial importance of density-dependent habitat selection in creating spatial patterns in the distribution and abundance of organisms.

Theory

The Model

Assume a population of identical individuals with discrete generations occupying two habitats. One habitat is of high-quality and the other of low-quality. Fitness in each habitat declines linearly with increasing density following the Ricker (1954) model of population growth:

$$N_{i(t+1)} = N_{i(t)}e^{r_i - b_i N_{i(t)}} \tag{1}$$

where N is population size in habitat i at times t and $t + 1$, r is the intrinsic rate of population growth and b is the strength of density-dependence. Converting equation (1) to natural logarithms linearizes fitness $\{\ln N_{i(t+1)} - \ln N_{i(t)}\}$ with density:

$$\ln N_{i(t+1)} - \ln N_{i(t)} = r_i - b_i N_{i(t)}.$$

If individuals select between the two habitats in order to maximize fitness, and are free to occupy their choice, they achieve an ideal-free distribution (IFD, Fretwell and Lucas 1969):

$$r_2 - b_2 N_2 = r_1 - b_1 N_1. \tag{2}$$

Rearranging equation (2) to solve for N_2 provides the linear ideal-free habitat isodar, the sets of densities in each habitat that equalize mean fitness between the two habitats at all population sizes:

$$N_2 = \frac{r_2 - r_1}{b_2} + \frac{b_1}{b_2}N_1. \tag{3}$$

Equation (3) demonstrates that quantitative (r_i) differences between habitats can yield sole occupation of the high-quality habitat below a threshold population size (IFD, Fig. 1a). Beyond this threshold, individuals also occupy low-quality habitat, but the frequency

of individuals in each one varies with population size. When individuals are unrelated, the isodar is an ESS (Cressman and Křivan 2006) and adaptive dispersal is halted.

However, such a strategy does not maximize per capita population growth rate when individuals are related. Related individuals that maximize inclusive fitness through habitat selection should sacrifice individual fitness for the benefit of relatives (MAXN, Morris et al. 2001, Morris 2011a). Dispersal among habitats will cease for the MAXN strategy when:

$$N_2 = \frac{r_2 - r_1}{b_2(1+R)} + \frac{b_1}{b_2} N_1 \tag{4}$$

where R is the coefficient of relatedness ($0 \leq R \geq 1$) of individuals, valued at 1 for clones (Morris et al. 2001). If individuals are identically related, the threshold for sole occupation of high-quality habitat is halved, and the low-quality habitat is occupied at a smaller population size than at the IFD equilibrium (Fig. 1a).

A linear decline in fitness with increasing density assumes that each individual has an equal effect on fitness at all population sizes: competition is independent of density. But this may not always be the case, and it is likely that density-dependence might often decelerate with increasing population size. For instance, competition for resources that is low at small population sizes is likely to intensify in large populations when the cumulative interactions with many competitors increase the proportion of consumed resources allocated to non-reproductive (competitive) activities. One effective way to capture these effects is to model fitness with a phenomenological version of a discrete-time Gompertz (1825) equation used by Dennis et al. (2006):

$$N_{i(t+1)} = N_{i(t)} e^{r_i - b_i \ln N_{i(t)}}. \tag{5}$$

Simplifying and equating fitness between habitats and rearranging to solve for N_2 yields the curvilinear ideal-free habitat isodar (Appendix A):

$$N_2 = e^{\frac{r_2 - r_1}{b_2}} N_1^{\frac{b_1}{b_2}} \tag{6}$$

and incorporating the effect of relatedness in maximizing inclusive fitness yields the MAXN strategy (Appendix A):

$$N_2 = [e^{r_2}(1 - Rb_2)]^{\frac{1}{b_2}} \left[e^{r_1} N_1^{-b_1}(1 - Rb_1)\right]^{\frac{1}{-b_2}}. \tag{7}$$

Unlike the linear isodars derived from the Ricker model, the Gompertz model yields steep isodars with subtle convex curvature and no threshold for sole occupation of high-quality habitat (Fig. 1b). Relative to the IFD, the MAXN strategy is no longer restricted to over-occupation of low-quality habitat (Fig. 1a vs Fig. 1b). A particularly interesting solution to equation (7) emerges with high levels of genetic relatedness and density-dependence ($b_i \geq 1$). The isodar is undefined. Thus, as population size increases, individuals have no habitat to occupy and maximize inclusive fitness by self-sacrifice. In cannibalistic species such as *F. candida*, a self-sacrificing individual provides nourishment to kin which can then be allocated towards future reproduction. It is unclear how frequent such an apparently paradoxical "ouroboros ESS" might be, but one cannot discount contemplating its existence.
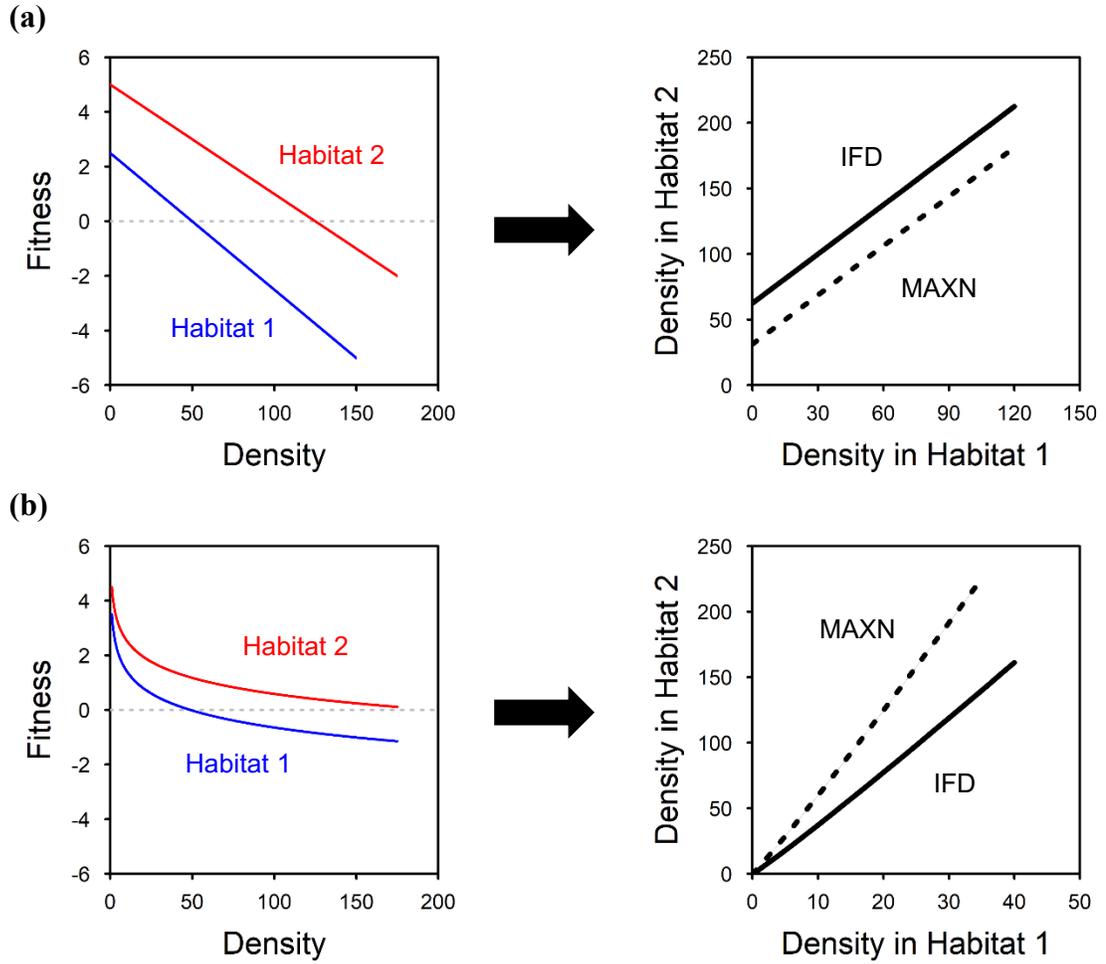
Figure 1. The relationship between fitness and density in two habitats (left panels) and the emerging strategies of habitat selection (right panels) for the ideal free distribution (IFD) and inclusive fitness strategy (MAXN; $R = 1$). (a) fitness functions calculated with the Ricker model ($r_1 = 2.5$ and $b_1 = 0.05$; $r_2 = 5$ and $b_2 = 0.04$), and (b) fitness functions calculated with the Gompertz model ($r_1 = 3.5$ and $b_1 = 0.9$; $r_2 = 4.5$ and $b_2 = 0.85$).

Testing the Model

I test whether the MAXN strategy yields higher population growth than does the IFD in clonal populations of *F. candida* given a choice between habitats of contrasting quality. I seek to answer three questions: (1) does the Gompertz model reveal differences among habitats in the relationship between fitness and density? (2) does habitat selection by *F. candida* fit the isodars expected by those relationships? and (3) do *F. candida* select habitat in a way that maximizes inclusive fitness (MAXN)?

I answer the questions with clones of *F. candida* descended from a single ancestor. I create high- to low-quality habitats by manipulating substrate moisture concentrations and inoculate each with *F. candida* across a range of population sizes. I fit the relationship between fitness and density in each of these control habitats with the Gompertz model of population growth. I use those relationships to calculate the IFD and MAXN isodars expected for animals choosing between pairs of habitats that differ in quality. I also allow populations of different sizes to select between the two habitats, measure the fitness accrued by those choices, then contrast their actual distribution and fitness with those expected from the control habitats.

Methods

Study Population

     Folsomia candida is a well-studied, exclusively female, parthenogenetic hexapod that is often used in eco-toxicological research (Pedersen et al. 2000, Fountain and Hopkin 2005). I used populations acquired from Dr. G. Boiteau at the University of New Brunswick. *F. candida* has a typical lifespan of 111 to 240 days at 15°C and 24°C respectively, while reaching maturity between 21 and 24 days (Fountain and Hopkin 2005). Females undergo approximately 45 moults in their lifetime, casting off their cuticles every three to four days until their 6th instar, and every five days thereafter (Snider 1973).

     Reproduction depends on density. Crowding (> 1 animal·cm^{-2}) reduces egg-laying (Green 1964, Fountain and Hopkin 2005). Mean clutch sizes vary from about 30 to 50 eggs which take seven to ten days to hatch (Fountain and Hopkin 2005). Reproduction occurs via infection of eggs by the parasitic bacterium *Wolbachia* (Riparbelli et al. 2006) inducing automictic parthenogenesis (Stenberg and Saura 2009). Terminal fusion during meiosis causes reproduction to be functionally mitotic (Ma and Schwander 2017) with potential to create clonal lineages (Tully et al. 2006) favouring the evolution of altruistic strategies.

     F. candida is a density-dependent habitat selector, and individuals select habitat contingent on their energetic state (Bannister and Morris 2016). *Folsomia* stressed by desiccation initiate sugar and polyol production to help maintain water balance (Bayley and Holmstrup 1999) likely at a cost to reproduction. When the stress is severe, it yields high rates of mortality. *F. candida* can identify and disperse to moist habitat when

exposed to mixtures of moist versus dry substrate (Joosse and Groen 1970, Verhoef and

van Selm 1983, Bannister and Morris 2016). Individuals tend to aggregate through

conspecific attraction (Verhoef et al. 1977, Nilsson and Bengtsson 2004), elicited by

olfactory sensing of fatty acids stored in the animal's cuticles (Liu and Wu 2017), but

show no evidence of social structure or social behaviour (Amorim et al. 2005).

Cannibalistic feeding on eggs (Fountain and Hopkin 2005) and conspecifics (Negri 2004)

reduces individual fitness. Cannibalism is particularly interesting in my experiments

because animals, and their eggs, are identically related. Individuals that consume eggs

and conspecifics are, like ancient Egypt's ouroboros iconograph, eating themselves.

Animal Cultures and Experiments

I maintained *F. candida* cultures in sealed plastic chambers (approx. 24 cm × 16

cm) with substrate consisting of a 9:1 ratio (by weight, ISO 1999) of plaster of Paris and

activated charcoal, and a 1:1 plaster to distilled water ratio by volume. I kept cultures in

constant darkness at room temperature (21°C ± 1.0 °C) to maximize egg production

(Fountain and Hopkin 2005). I fed animals in the chambers approximately 60 pellets of

baker's yeast (Fleischmann's ® traditional active dry yeast) and maintained (100%)

substrate moisture concentrations by adding 5 mL of distilled water, weekly.

I created a clonal culture (K1) of animals from a single founding mother using

eggs laid on June 14, 2017. I allowed adults in the K1 lineage to lay eggs in 13 chambers

for seven days to create a large age-synchronized culture. Age-synchronization produced

a discrete (seven day) period of reproduction assumed by my use of the Gompertz model.

I assumed an 8-day hatch time for eggs laid on each of the seven days of reproduction

and allowed age-synchronized animals to mature 24 (youngest) to 30 (oldest) days in

each chamber. I then transferred all age-synchronized animals into a single large chamber (approx. 42 cm × 29 cm) with superabundant food. I created experimental populations four days later (animals aged 28 to 34 days) with random subsamples to minimize inter-individual variation in reproductive output (Axelsen et al. 1998, Crouau and Cazes 2003). I transferred these populations into 100-mm × 15-mm polystyrene disposable petri dishes which I sealed with parafilm for experiments. One set of dishes served as controls (a single habitat) and another set allowed choice between two habitats. I repeated this protocol to create four age-synchronized experimental cohorts between May 24 and July 15, 2018 (Table B1).

I created controls by pouring substrate into single petri dishes (Appendix C1). I allowed animals to choose between habitats by pouring substrate into petri dishes divided into three compartments: two distinct habitats adjacent to a central release site (Appendix C1). I attached the release site, a 50-mm × 9-mm BD Falcon petri dish lid, centrally in the large petri dish using all-purpose silicone caulking. I connected the lid to an impermeable caulking barrier to partition the large dish into two periphery habitats of equal size (Fig. C1).

I used four substrate moisture concentrations to create habitats of varying quality because of *F. candida*'s potential metabolic trade-off between survival and reproduction in the face of desiccation: high-quality (100% water saturation, Appendix C2), moderate-quality (37.5% water saturation), moderately-low-quality (25% water saturation), and low-quality (12.5% water saturation). No adults survived, and no eggs were laid, in experimental dishes with less than 12.5% water saturation (Appendix C3). There was no mortality and minimal egg production between 12.5% and 37.5% water saturations. I was

unable to distinguish survival or reproductive differences among dishes with saturation levels above 37.5% (all high-quality habitat, Appendix C3).

Habitat Selection

All experiments used petri dishes that paired high-quality habitat (100% water saturation) with all alternative habitats (12.5, 25, 37.5 and 100% saturation respectively). I labelled the bottom of each dish as 1 or 2 to represent either high- or low-quality habitat. Doing so also allowed me to always choose the same side for comparing densities and fitness in dishes with only 100% water saturations. I populated each petri dish's central release site (also 100% water saturation) with 40 to 800 8th instar (28- to 34-day-old) individuals of *F. candida* in increments of 40 (20 populations for each pair of habitats). I was unable to monitor all 80 populations simultaneously (33,600 animals in total), so I chose five different population sizes from each of the four age-synchronized cultures to run simultaneously (20 populations, 5 in each of the four different habitat pairings, Table B1). I completed all experiments in 164 days.

I allowed animals to disperse for 24 hours. The 24-hour period was sufficient for animals to move throughout the petri dishes (Auclerc et al. 2010) and to reach a stable distribution of individuals in each habitat (Bannister and Morris 2016). I photographed each petri dish at 24 hours at a constant distance and angle with an 8-megapixel camera (iPhone 6), then immediately transferred populations to new dishes with a single etched (to facilitate egg laying) habitat identical in substrate moisture concentration to their habitat choice. I displayed the photographs on a computer monitor and counted the number of individuals in each habitat for each of the 20 populations. I converted

abundances to densities standardized to the area of whole petri dishes (58 cm^2, Appendix C4) and used those values to generate habitat isodars.

Fitness and Density

I used animals living in control dishes within a single homogeneous habitat to determine the relationships between fitness and density. The number of populations and total population sizes were identical to those I used to evaluate habitat selection, plus four additional population sizes (10, 20, 900 and 1000 animals, Table B1; 41,320 animals in total) that I used to better characterize the curvature of density-dependence emerging at very low and high densities (Fig. 2). I synchronized control and habitat-selecting populations aged 28 to 34 days (8th instar) by placing control animals in completely saturated habitat dishes (100%, no compartments) without food while habitat-selection populations chose habitat (also without food). I transferred populations from both experiments 24 hours later to their respective homogeneous habitats for nine days in order to eliminate state-dependent carryover effects associated with initial culture conditions (Wallenstein and Fisher 1977, Norris 2005, Harrison et al. 2011, O'Connor et al. 2014, Bannister and Morris 2016). I placed a single yeast pellet in the centre of every dish. I transferred these populations (now in their 10th instar) to new dishes with the same etched habitat for another nine days to lay eggs. I then removed adults to simulate a semelparous life history and create discrete generations to fit the Gompertz model of population growth. I allowed all eggs to hatch. I renewed moisture (with a micropipette) and the yeast pellet weekly (Appendix C5), along with the removal of eggs laid by recruits between 6th and 10th instars. I photographed each dish as above, displayed the

images on a computer monitor, and used the count of individuals reaching the 10th instar as my estimate of density.

Statistical Analysis

Fitness and Density

I used natural logarithms to linearize equation (5) as

$$\ln N_{i(t+1)} - \ln N_{i(t)} = r_i - b_i \ln N_{i(t)} \tag{8}$$

and estimated maximum population growth (r_i) and density-dependence (b_i) with least-squares regression. To discount differences in sample size between control ($n = 24$) and habitat-selection populations ($n = 20$, except in the lowest quality habitat where extinction of a population with only 3 animals reduced the number of replicates to 19), I resampled 20 of the 24 control data points without replacement to create 10,000 'bootstrapped' regressions. I evaluated whether the intercepts and slopes from the analysis of the original data fell within the 95% confidence interval of these estimates. Sample sizes were disproportionately larger in high-quality habitat ($n = 100$) because each habitat-selection petri dish included that habitat. I investigated whether mean fitness achieved in these high-quality habitats differed among populations with a general linear model (GLM).

Habitat Selection

I created empirical isodars by regressing density in high-quality (100%) habitat against the respective density in each alternative habitat. I transformed all density values to natural logarithms in order to conform with the linearized Gompertz expectation (e.g., for the IFD):

$$\ln N_2 = \frac{r_2 - r_1}{b_2} + \frac{b_1}{b_2} \ln N_1. \tag{9}$$

I analyzed each isodar with standard major axis regression (Morris 1987; 'smatr' package in R software, Warton et al. 2012, R Development Core Team 2013).

I calculated IFD and MAXN isodars for each set of paired-habitats from the corresponding control fitness functions using equations (6) and (7) respectively. I used the isodar solutions to predict the density of animals that should occupy high-quality habitat for every density that habitat selectors achieved in alternative habitats. These predictions often yielded partial individuals, so I rounded predictions to the nearest integer. As with empirical isodars, I transformed all density values to their natural logarithms and analyzed each expected isodar with standard major axis regression. I complemented this analysis by calculating the mean fitness expected from all possible combinations of animals selecting each habitat for each population size in each of the four habitat-selection treatments. I then determined which combinations minimized differences between habitats in expected fitness (corresponds with an IFD), and which maximized total population growth (MAXN). I completed my analysis by testing whether the fitness $\{\ln N_{i(t+1)} - \ln N_{i(t)}$, left-hand term in equation (8)$\}$ achieved by habitat-selecting *F. candida* best corresponded with IFD or MAXN expectations (one-sample t-tests on the difference between empirical and expected values).

Results

Fitness and Density

The range of densities in lower-quality habitats was consistently less for animals allowed to choose between habitats than it was in controls (Fig. 2). Fitness, and its relationship with density, differed among habitats and between control and habitat-selection experiments (Fig. 2). Fitness in the saturated (100%) habitat was much higher at all densities than in the low-quality (12.5%) habitat where fitness was also more variable (Fig. 2, Table 1).

I used these fitness-density relationships to compare empirical and predicted isodars. But first I used three different tests to confirm that the control experiments were appropriate for predicting IFD and MAXN habitat selection, and subsequent fitness.

I began with my bootstrapped test evaluating whether reducing sample size from $n = 24$ to $n = 20$ influenced the relationships between fitness and density in each experiment. Differences in sample size had no significant effect on those relationships (all intercepts and slopes were well within the confidence intervals of, and nearly identical to, estimates from the resampled data, Table 1). Next, I tested whether mean fitness of habitat-selecting populations occupying high-quality habitat (100%) differed among each two-habitat comparison. There was no difference in mean fitness in high-quality habitat among the habitat-selection experiments ($F_{3,95} = 1.03$, $P > 0.4$, GLM) even though the number of animals choosing the 100% habitat varied for each comparison.

I completed my tests by assessing the sensitivity of control fitness data to their long high-density tails (Fig. 2). I did so by successively deleting the highest-density data point (one-at-a-time), then re-calculating the fitness functions for each iteration.

Parameter values of the fitness functions were relatively invariant (maximum change =

0.24; Table D1) even when shortened to only the 11 lowest-density ($N_t \approx 350$) data

points. I re-calculated expected isodars using the most extreme control fitness functions.

These rarified isodars yielded the same outcomes as those generated from the full data

sets in 3 out of 4 cases (Table 2). But in the high- vs moderate-quality (100% vs 37.5%)

habitat comparison, the MAXN strategy shifted towards empirical and IFD expectations

(Fig. D1). Regardless of this convergence, the relative positions and slopes of the isodars

were identical to those predicted from the full data set, so I retained the full data for

subsequent analyses.

Table 1. Least-squares linear regressions of fitness on density in four habitats (% water saturation) occupied by cloned populations of *Folsomia candida* in control and habitat selection experiments. Mean values and lower (L) and upper (U) 95% confidence intervals provided for 10,000 resampled (20/24) sets of control fitness data.

Experiment	Habitat	Intercept	Resampled Intercept			Slope	Resampled Slope			R^2	P
			Mean	L	U		Mean	L	U		
Control	100% ($n = 24$)	4.74	4.72	4.25	5.16	-0.81	-0.81	-0.88	-0.70	0.87	< 0.001
	37.5% ($n = 24$)	5.26	5.25	4.89	5.67	-0.96	-0.96	-1.02	-0.89	0.92	< 0.001
	25% ($n = 24$)	3.78	3.79	3.22	4.24	-0.72	-0.72	-0.79	-0.62	0.85	< 0.001
	12.5% ($n = 24$)	3.90	3.93	2.95	5.46	-1.05	-1.06	-1.32	-0.90	0.56	< 0.001
Habitat selection	100% ($n = 100$)	4.94	-	-	-	-0.86	-	-	-	0.87	< 0.001
	37.5% ($n = 20$)	4.76	-	-	-	-0.85	-	-	-	0.91	< 0.001
	25% ($n = 20$)	5.23	-	-	-	-0.95	-	-	-	0.93	< 0.001
	12.5% ($n = 19$)	3.81	-	-	-	-0.85	-	-	-	0.68	< 0.001

Figure 2. Relationships between fitness ($\ln N_{t+1}$ - $\ln N_t$) and density in each of four habitats occupied by *Folsomia candida* in control (C, red) and habitat selection (HS, blue) experiments. Equations represent transformed data (natural logarithms) solved with least-squares linear regression.
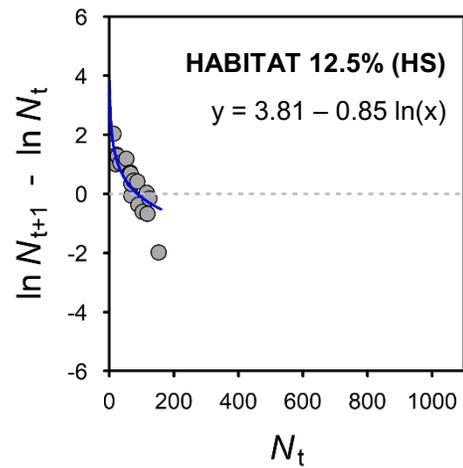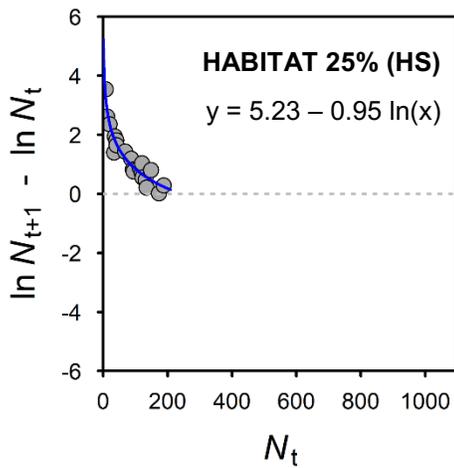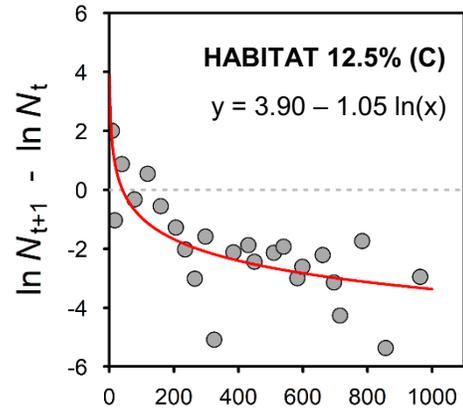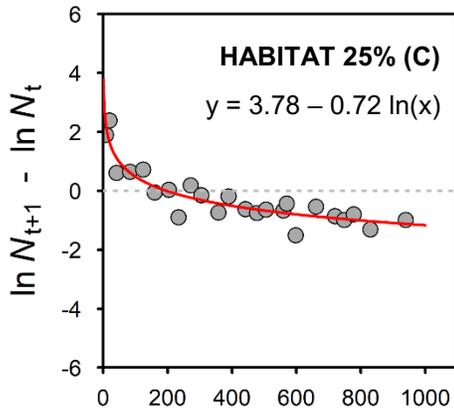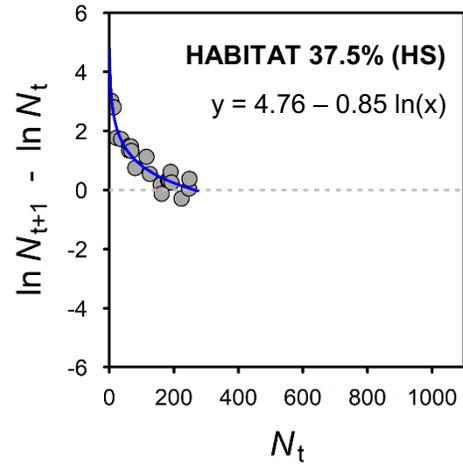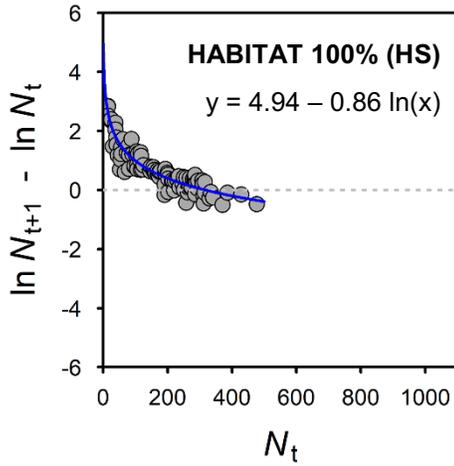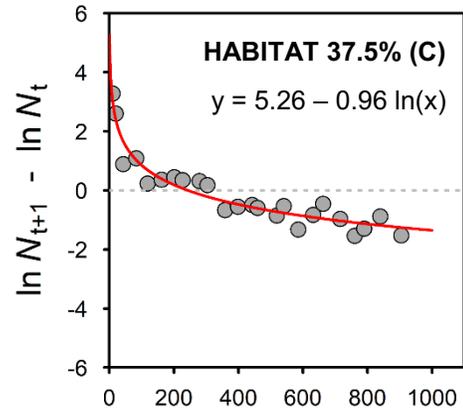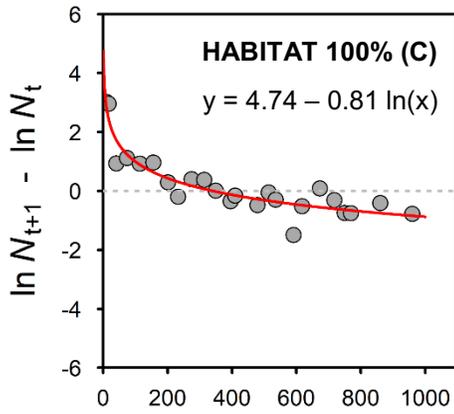
Habitat Selection

All isodar regressions were highly significant and confirmed the expectation that more individuals should occupy high- than low-quality habitat (Fig. 3). Isodar intercepts tended to be higher, and their slopes shallower, than expected by controls (Table 2). Empirical and expected isodars were similar in dishes composed of two identical habitats (100% moisture concentration), and in dishes enabling selection between high- (100%) and moderate-quality (25%) habitats (Fig. 3). Intercepts of empirical isodars were higher than IFD predictions, and their slopes lower, in dishes containing 37.5% and 12.5% moisture habitats.

Comparisons of all possible distributions of individuals among habitat pairs were surprising. All IFD solutions yielded a single strategy (one pair of densities) at each population size (Fig. 4). But the MAXN solutions yielded an increasingly wide range of density-pairs that produced identical maximum population sizes in the next generation (equal population growth). A clear example is the MAXN solution contrasting high-versus moderately-low-quality habitats (100% vs 25% moisture, Fig. 4). The existence of multiple 'strategies' yielding identical outcomes is intriguing because it demonstrates the potential for a variety of isodars that can diverge from one another, or meander among alternatives at different population sizes (Fig. 4). The cloud of possible isodars should nevertheless cluster around the theoretical isodar (MAXN) predicted from equation (7).

Table 2. Empirical and expected habitat isodars (IFD and MAXN from controls) of clonal *Folsomia candida* choosing between habitats varying in moisture concentration. All isodars based on standard major axis regressions of logarithmically (ln) transformed density. Lower (L) and upper (U) 95% confidence intervals provided for empirical isodars. Parameter values provided in brackets for rarified expected isodars. * = an expectation that only 1 individual should occupy the low-quality habitat (Fig. 3).

Habitat Comparison (% moisture)	Empirical Isodars				Expected Isodars			
					IFD		MAXN	
	Intercept	Slope	R^2	P	Intercept	Slope	Intercept	Slope
100 vs 100 (*n* = 20)	-0.22 L (-1.08) U (0.64)	1.00 L (0.86) U (1.15)	0.91	< 0.001	0 (0)	1 (1)	0 (0)	1 (1)
100 vs 37.5 (*n* = 20)	1.68 L (0.89) U (2.47)	0.73 L (0.60) U (0.88)	0.86	< 0.001	-0.64 (-0.30)	1.18 (1.10)	1.19 (0.47)	1.18 (1.10)
100 vs 25 (*n* = 20)	1.06 L (0.12) U (2.00)	0.91 L (0.75) U (1.09)	0.85	< 0.001	1.18 (1.13)	0.88 (0.90)	0.67 (0.68)	0.88 (0.90)
100 vs 12.5 (*n* = 20)	2.46 L (1.61) U (3.31)	0.72 L (0.57) U (0.91)	0.78	< 0.001	1.03 (0.83)	1.29 (1.36)	0 (0)	* (*)
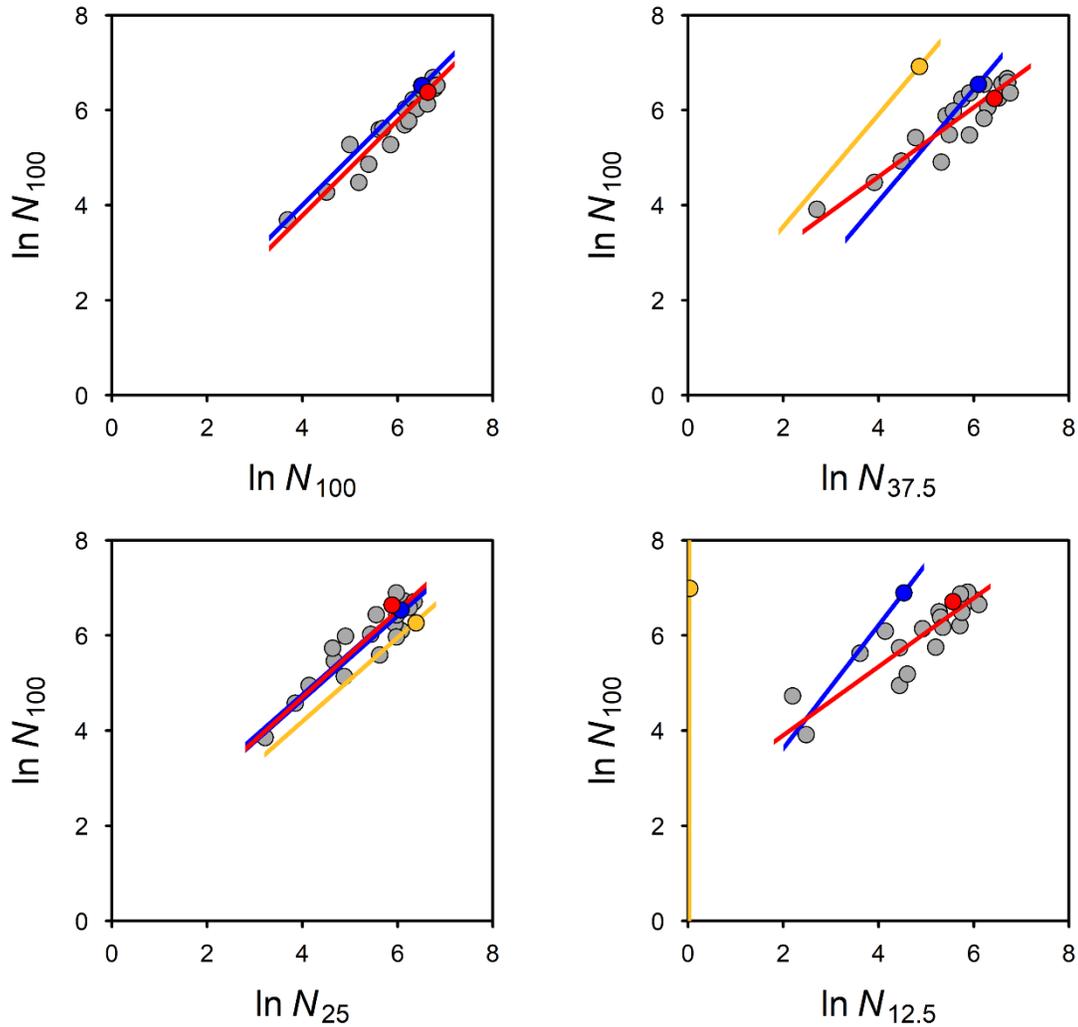
Figure 3. Empirical (red, shaded circles) and expected IFD (blue) and MAXN (gold) isodars of *Folsomia candida* populations occupying petri dishes with four different pairs of habitats varying in moisture concentration. Red, blue, and gold circles (empirical, IFD, and MAXN respectively) represent fits to each isodar for the same total population size (100% vs 100% = 1351; 100% vs 37.5% = 1139; 100% vs 25% = 1121; 100% vs 12.5% = 1080). IFD and MAXN expectations are identical in the control comparison (both 100%), the expected MAXN isodar is vertical in the most extreme pair of habitats (one individual in the 12.5% moisture habitat). All empirical isodars based on standard major axis regressions of logarithmically transformed density, $\ln N_t$.
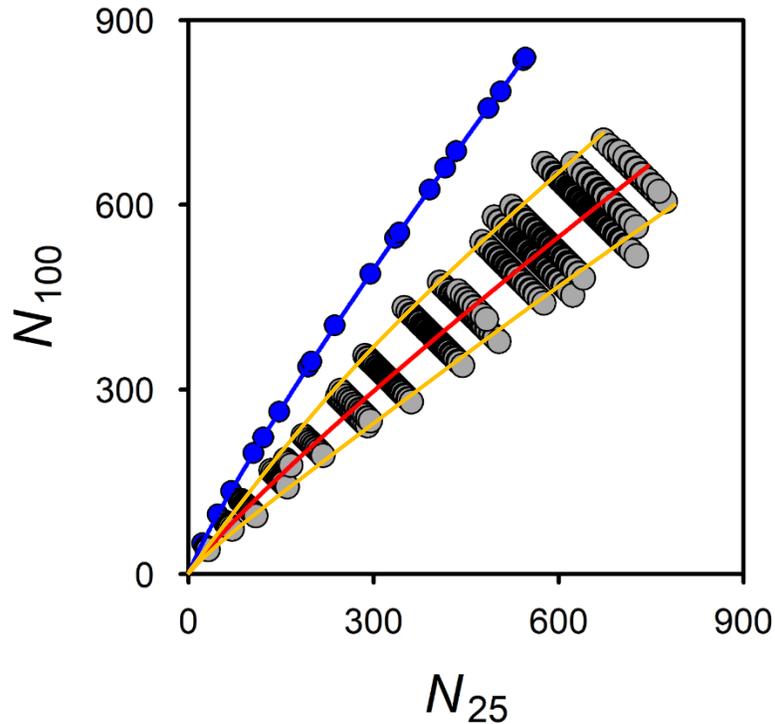
Figure 4. Expected IFD and MAXN isodars for *Folsomia candida* choosing between high- versus moderately-low-quality (100% vs 25%) habitats. Circles represent IFD (blue) and MAXN (grey) isodar solutions based on all possible comparisons of density (*N*) at 20 different population sizes. Blue and red lines correspond with solutions (from Fig. 2) to equations (6, IFD) and (7, MAXN) respectively. Gold lines represent two of many different possible MAXN isodars that yield identical population growth.

Empirical isodars tended to be more similar to expectations of the IFD than to those of the MAXN (Fig. 3). So I used a two-tailed paired t-test to evaluate whether mean fitness was greater in one habitat than in the other. I subtracted fitness in lower-quality habitat from fitness in high-quality (100%) habitat (side 1 minus side 2). Those values were not different from zero (IFD) when animals chose between habitats of equal quality (100%), or when they chose between extreme habitats (100% vs 12.5%). Mean fitness

was higher in the 37.5% and 25% habitats than in their respective high-quality alternative choices (Table 3; Fig. 5). This pattern did not depend on population size (GLM, $F_{1,36}$ = 0.20, P = 0.7). Regardless, population growth achieved by habitat-selecting *F. candida* was at least as high, or higher (100% vs 25% comparison), than the values expected by either the IFD or MAXN solutions (Fig. 6).

Table 3. Mean differences and 95% confidence intervals of two-tailed paired t-tests assessing fitness differences between pairs of habitats chosen by *Folsomia candida*.

Habitat Comparison (% moisture)	Fitness Differences				
	Mean	95% CIs		t	P
		Lower	Upper		
100 vs 100 (*n* = 20)	-0.09	-0.22	0.04	-1.38	0.2
100 vs 37.5 (*n* = 20)	-0.30	-0.51	-0.09	-3.00	0.007
100 vs 25 (*n* = 20)	-0.55	-0.78	-0.32	-4.96	< 0.001
100 vs 12.5 (*n* = 19)	-0.08	-0.43	0.27	-0.47	0.6
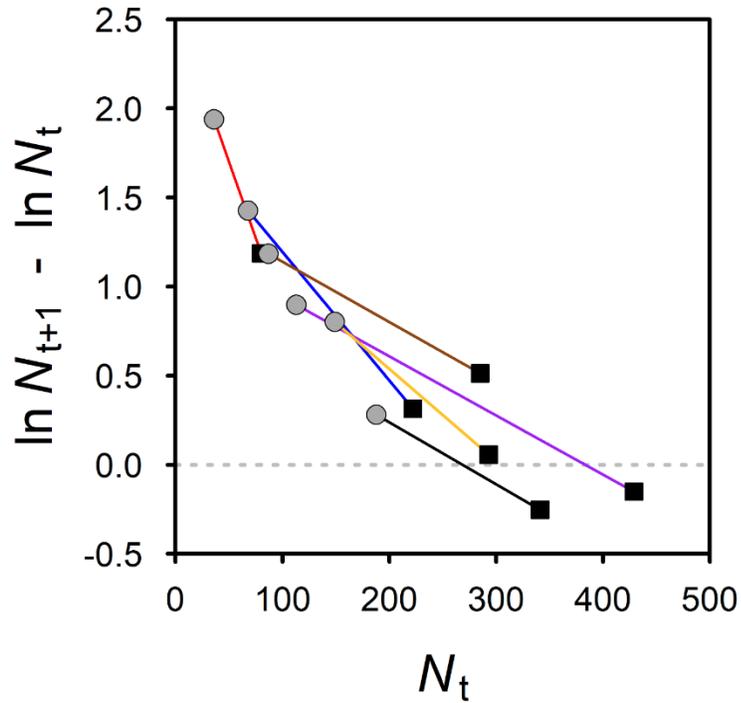
Figure 5. A subset (6 of 20) of the fitness achieved by clonal *Folsomia candida* populations choosing between high- versus moderately-low-quality (100% vs 25%) habitats. Lines connect densities in low-quality (25%, shaded circles) with densities in high-quality (100%, black squares) habitat at six different population sizes (116, 290, 372, 542, 442, and 529 respectively).
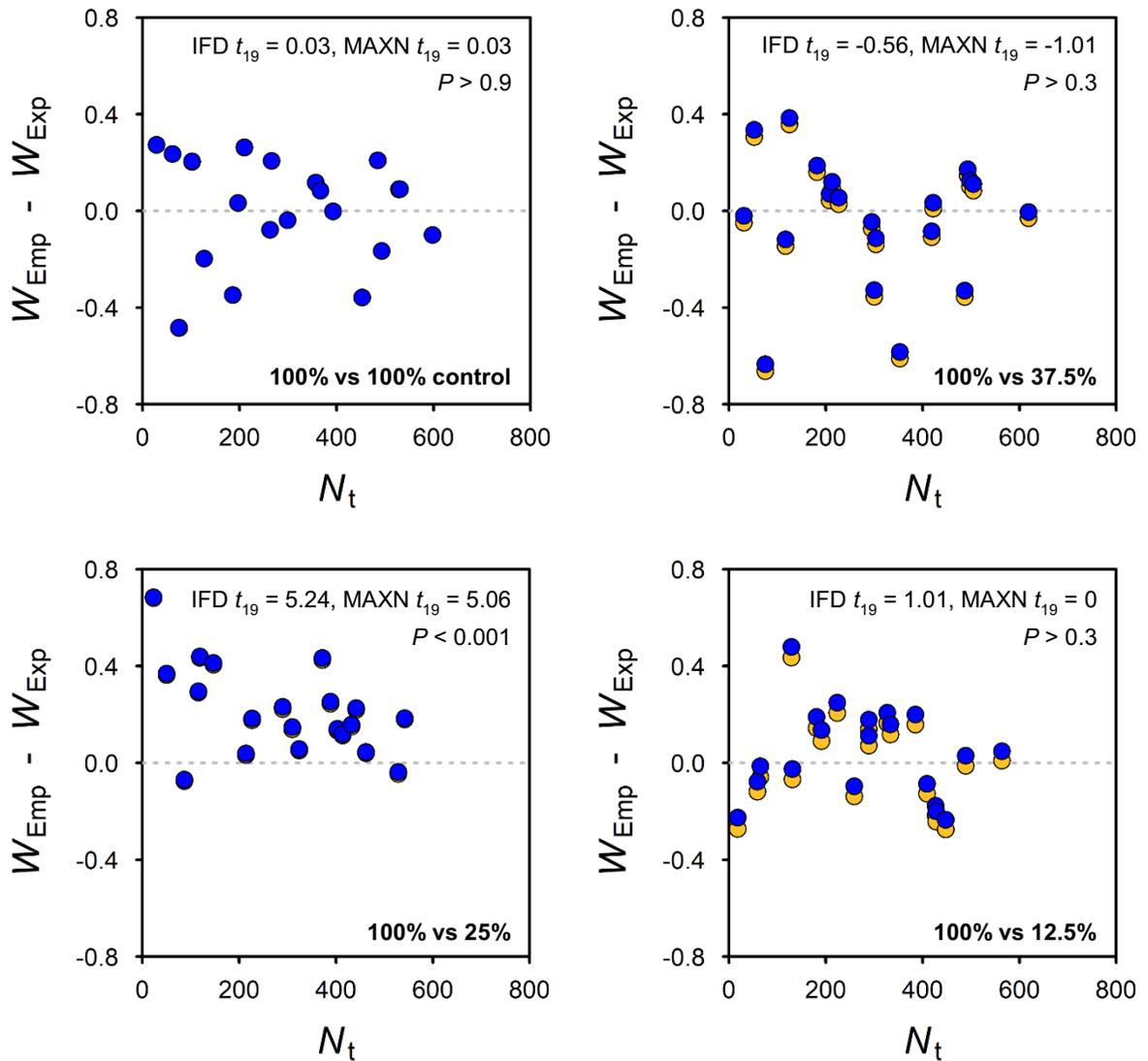
Figure 6. Mean fitness (W) differences between empirical and expected isodars (IFD = blue, MAXN = gold; gold and blue data points overlap one another in both left-hand panels) by habitat-selecting *Folsomia candida* populations occupying four different habitats varying in moisture concentration and initial population size, N_t (two-tailed one sample t-test statistics and significance values provided). Mean fitness weighted by the densities in each habitat.

Discussion

Clonal populations of *F. candida* maximized fitness through habitat choice. This important result emphasizes the point made by Moses et al. (2013) that if "simple" organisms can achieve an ESS of habitat selection, one can anticipate that others should too. But *F. candida* habitat selection provides an additional crucial insight into our understanding of the ESS. Habitat-selecting hexapods altered the very relationships between density and fitness that determine the ESS and subsequent population growth. It is tempting to suggest that habitat-selecting *F. candida* anticipated their newly defined fitness functions, but it is most likely that patterns in fitness arose through habitat choice. The implication is that different 'classes' of animals occupied the two habitats. Otherwise, there should have been no difference between fitness functions generated by control versus habitat-selecting *Folsomia.* The pronounced effect of habitat selection on a habitat's fitness is all the more remarkable because my clonal populations excluded the potential influence of genetics on habitat choice.

It is tempting to suggest that some other aspect of the organisms' state must be responsible for habitat preference. The problem with that suggestion is that my experiments controlled for state-dependence with synchronized cultures growing under identical conditions prior to habitat selection. Be that as it may, the lesson is clear. Predictions of future patterns in abundance and distribution are likely to be incorrect if they fail to account for the emergent strategies (isodars) associated with habitat choice.

Another intriguing outcome is that the MAXN strategy for convex fitness functions yields numerous possible isodar solutions (e.g., Fig. 4). The loss in contributing to population growth in one habitat is perfectly compensated by the gain in population

growth achieved by occupying the second habitat. The resultant potential for multiple

isodars (or more generally, a more variable isodar) limits the possibility to differentiate

between cooperative (MAXN) and selfish (IFD) strategies of habitat selection.

My tests of habitat selection by *F. candida* demonstrate the importance of testing

theory with experiments that yield *a priori* predictions of habitat preference. Fitness and

habitat preference clearly depended on substrate moisture concentrations. I used those

relationships to determine the optimal habitat occupation predicted by two divergent

models of habitat selection. Neither was correct because the animals chose their habitats

differently. Their strategy, paradoxically, yielded higher fitness in low-quality habitat

than it did in the high-quality habitat. But the paradox is only apparent because the

strategy yielded population growth rates equal to, or exceeding, those predicted from

controls. Theory explains why. Convex relationships between fitness and density yield

new and unexpected patterns of spatial abundance and distribution, including the

possibility that habitat-selecting relatives can maximize their inclusive fitness by suicide

and self-cannibalism (consuming eggs). Cannibalism might thus represent the otherwise

unexplained state-dependence in habitat choice. The novel patterns of distribution

associated with curved fitness functions are especially important because concave upward

(= convex) relationships between population growth rate and density are prevalent across

major taxonomic groups of animals (Sibly et al. 2005).

The potential proximate causes of habitat choice by *F. candida* are no less

intriguing than are the evolutionary strategies associated with an optimal distribution

between habitats. *F. candida* are attracted to conspecific fatty-acids (Liu and Wu 2017).

The attraction is likely to represent a form of public information (Valone 1989, Danchin

et al. 2004) that the animals can use as an indirect cue of habitat quality. If that cue also depends on density, then it should help to explain why both density and fitness are altered by habitat choice.

One might be tempted to interpret my experiments as a halcyon call to measure fitness in all studies of habitat selection. Doing so would undermine its main contribution. Habitat isodars are the ESS of density-dependent habitat selection that provide deep insights into population dynamics and the structure of ecological communities (Morris 1988). With anthropogenic-induced habitat loss, destruction, and fragmentation being primary drivers of global species population decline (Krause et al. 2010, Haddad et al. 2015, Newbold et al. 2015, Deinet et al. 2018), there is an urgency, now more than ever, to use our knowledge of habitat selection to better understand the dynamic interaction between ecology and evolution, and to more effectively invoke strategies for the conservation of biodiversity.

References

Amorim, M. J. B., J. Römbke, A. Scheffczyk, A. J. A. Nogueira, and A. M. V. M Soares. 2005. Effects of different soil types on the collembolans *Folsomia candida* and Hypogastrura assimilis using the herbicide phenmedipham. Archives of Environmental Contamination and Toxicology 49:343–352.

Auclerc, A., P. A. Libourel, S. Salmon, V. Bels, and J. F. Ponge. 2010. Assessment of movement patterns in *Folsomia candida* (Hexapoda: Collembola) in the presence of food. Soil Biology and Biochemistry 42:657–659.

Axelsen, J. A., M. Holmstrup, and P. H. Krogh. 1998. Simulation of development and reproduction of Collembola sampled from synchronized cultures. Pedobiologia 42:1–9.

Bannister, A. E., and D. W. Morris. 2016. Habitat selection reveals state-dependent foraging trade-offs in a temporally autocorrelated environment. Israel Journal of Ecology and Evolution 62:162–170.

Bayley, M., and M. Holmstrup. 1999. Water vapour absorption in arthropods by accumulation of myoinositol and glucose. Science 285:1909–1911.

Cressman, R., and V. Křivan. 2006. Migration dynamics for the ideal free distribution. American Naturalist 168:384–397.

Crouau, Y., and L. Cazes. 2003. What causes variability in the *Folsomia candida* reproduction test? Applied Soil Ecology 22:175–180.

Danchin, E., L. A. Giraldeau, T. J. Valone, and R. H. Wagner. 2004. Public information: from nosy neighbors to cultural evolution. Science 305:487–491.

Deinet, S., L. McRae, and R. Freeman. 2018. Population indicator: the living planet

    index. Pages 88–95 *in* M. Grooten, and R. E. A. Almond, eds. Living planet report

    2018: aiming higher. World Wildlife Fund, Gland, Switzerland.

Dennis, B., J. M. Ponciano, S. R. Lele, M. L. Taper, D. F. Staples. 2006. Estimating

    density dependence, process noise, and observation error. Ecological Monographs

    76:323–341.

Fountain, M. T., and S. P. Hopkin. 2005. *Folsomia candida* (Collembola): a "standard"

    soil arthropod. Annual Review of Entomology 50:201–222.

Fretwell, S. D., and H. L. Lucas. 1969. On territorial behaviour and other factors

    influencing habitat distribution in birds. Acta Biotheoretica 19:45–52.

Gardner, A., and J.J. Welch. 2011. A formal theory of the selfish gene. Journal of

    Evolutionary Biology 24:1801–1813.

Gompertz, B. 1825. On the nature of the function expressive of the law of human

    mortality, and on a new mode of determining the value of life contingencies.

    Philosophical Transactions of the Royal Society of London B 115:513–585.

Green, C. D. 1964. The effect of crowding upon the fecundity of *Folsomia candida*

    (William) var. Distincta (Bagnall) (Collembola). Entomologia Experimentalis et

    Applicata 7:62–70.

Haddad, N. M., L. A. Brudvig, J. Clobert, K. F. Davies, A. Gonzalez, R. D. Holt, et al.

    2015. Habitat fragmentation and its lasting impact on Earth's ecosystems. Science

    Advances 1:e1500052.

Hamilton, W. D. 1963. The evolution of altruistic behaviour. American Naturalist

    97:354–356.

Harrison, X. A., J. D. Blount, R. Inger, D. R. Norris, and S. Bearhop. 2011. Carry-over effects as drivers of fitness differences in animals. Journal of Animal Ecology 80:4–18.

Holt, R. D. 1985. Population dynamics in two-patch environments: some anomalous consequences of an optimal habitat distribution. Theoretical Population Biology 28:181–208.

Holt, R. D. 1987. Population dynamics and evolutionary processes: the manifold roles of habitat selection. Evolutionary Ecology 1:33–347.

ISO. 1999. Soil quality-inhibition of reproduction of Collembola (*Folsomia candida*) by soil pollutants. (ISO 11267: 1-16). Geneva: International Standardization Organization.

Joosse, E. N. G., and J. B. Groen. 1970. Relationship between saturation deficit and the survival and locomotory activity of surface dwelling Collembola. Entomologia Experimentalis et Applicata 13:229–235.

Krause, J., R. Bommarco, M. Guardiola, R. K. Heikkinen, A. Helm, M. Kuussaari, et al. 2010. Habitat fragmentation causes immediate and time-delayed biodiversity loss at different trophic levels. Ecology Letters 13:597–605.

Liu, J., and D. Wu. 2017. Chemical attraction of conspecifics in *Folsomia candida* (Collembola). Journal of Insect Behaviour 30:331–341.

Ma, W. J., and T. Schwander. 2017. Patterns and mechanisms in instances of endosymbiont-induced parthenogenesis. Journal of Evolutionary Biology 30:868–888.

Maynard Smith, J. 1982. Evolution and the theory of games. Cambridge University Press, Cambridge, UK.

Morris, D. W. 1987. Tests of density-dependent habitat selection in a patchy environment. Ecological Monographs 57:269–281.

Morris, D. W. 1988. Habitat-dependent population regulation and community structure. Evolutionary Ecology 2:253–269.

Morris, D. W. 1989. Density-dependent habitat selection: testing the theory with fitness data. Evolutionary Ecology 3:80–94.

Morris, D. W. 2003a. Toward and ecological synthesis: a case for habitat selection. Oecologia 136:1–13.

Morris, D. W. 2003b. Shadows of predation: habitat-selecting consumers eclipse competition between coexisting prey. Evolutionary Ecology 17:393–422.

Morris, D. W. 2011a. Source-sink dynamics emerging from unstable ideal free habitat selection. Pages 58–81 *in* J. Liu, V. Hull, A. T. Morzillo, and J. A. Wiens, eds. Sources, sinks and sustainability. Cambridge University Press, Cambridge, UK.

Morris, D. W. 2011b. Adaptation and habitat selection in the eco-evolutionary process. Proceedings of the Royal Society B 278:2401–2411.

Morris, D. W., and D. L. Davidson. 2000. Optimally foraging mice match patch use with habitat differences in fitness. Ecology 81:2061–2066.

Morris, D. W., and P. Lundberg. 2011. Pillars of evolution: fundamental principles of the eco-evolutionary process. Oxford University Press, Oxford, UK.

Morris, D. W., D. L. Davidson, and C. J. Krebs. 2000. Measuring the ghost of competition: insights from density-dependent habitat selection on the co-existence and dynamics of lemmings. Evolutionary Ecology Research 2:41–67.

Morris, D. W., P. Lundberg, and J. Ripa. 2001. Hamilton's rule confronts ideal free habitat selection. Proceedings of the Royal Society B 268:921–924.

Morris, D. W., J. E. Diffendorfer, and P. Lundberg. 2004. Dispersal among habitats varying in fitness: reciprocating migration through ideal habitat selection. Oikos 107:559–575.

Moses, M. M., D. W. Morris, and W. Qin. 2013. Greener on the other side of the fence: density-dependent habitat selection by a unicellular alga. Evolutionary Ecology 15:809–828.

Negri, I. 2004. Spatial distribution of Collembola in presence and absence of a predator. Pedobiologia 48:585–588.

Newbold, T., L. N. Hudson, S. L. L. Hill, S. Contu, I. Lysenko, R. A. Senior, et al. 2015. Global effects of land use on local terrestrial biodiversity. Nature 520:45–69.

Nilsson, E., and G. Bengtsson. 2004. Endogenous free fatty acids repel and attract Collembola. Journal of Chemical Ecology 30:1431–1443.

Norris, D. R. 2005. Carry-over effects and habitat quality in migratory populations. Oikos 109:178–186.

O'Connor, C. M., D. R. Norris, G. T. Crossin, and S. J. Cooke. 2014. Biological carryover effects: linking common concepts and mechanisms in ecology and evolution. Ecosphere 5:1–11.

Pedersen, M. B., C. A. M. van Gestel, and N. Elmegaard. 2000. Effects of copper on reproduction of two Collembola species exposed through soil, food, and water. Environmental Toxicology and Chemistry 19:2579–2588.

R Development Core Team. 2013. R: a language and environment for statistical computing. R Foundation for Statistical Computing, Vienna, Austria. Retrieved from http://www.R-project.org/.

Ricker, W. E. 1954. Stock and recruitment. Journal of the Fisheries Research Board of Canada 11:559–623.

Riparbelli, M. G., R. Giordano, and G. Callaini. 2006. Centrosome inheritance in the parthenogenetic egg of the collembolan *Folsomia candida*. Cell Tissue Research 326:861–872.

Rodenhouse, N. L., T. W. Sherry, and R. T. Holmes. 1997. Site-dependent regulation of population size: a new synthesis. Ecology 2:2025–2042.

Rosenzweig, M. L. 1981. A theory of habitat selection. Ecology 62:327–335.

Sibly, R. M., D. Barker, M. C. Denham, J. Hone, and M. Pagel. 2005. On the regulation of populations of mammals, birds, fish, and insects. Science 309:607–610.

Snider, R. M. 1973. Laboratory observations on the biology of *Folsomia candida* (Willem) (Collembola: Isotomidae). Revue d'Ecologie et de Biologie du Sol 10:103–121.

Stenberg, P., and A. Saura. 2009. Cytology of asexual animals. Pages 63–74 *in* I. Schon, K. Martens, and P. van Dijk, eds. Lost sex: the evolutionary biology of parthenogenesis. Springer Science and Business Media, Netherlands.

Tregenza, T. 1995. Building on the ideal free distribution. Advances in Ecological
Research 26:253–302.

Tully, T., C. A. D'Haese, M. Richard, and R. Ferrière. 2006. Two major evolutionary
lineages revealed by molecular phylogeny in the parthenogenetic Collembola
species *Folsomia candida*. Pedobiologia 50:95–104.

Valone, T. J. 1989. Group foraging, public information, and patch estimation. Oikos
56:357–363.

Verhoef, H. A., and A. J. van Selm. 1983. Distribution and population dynamics of
Collembola in relation to soil moisture. Holarctic Ecology 6:387–394.

Verhoef, H. A., C. J. Nagelkerke, and E. N. G. Joosse. 1977. Aggregation pheromones in
Collembola. Journal of Insect Physiology 23:1009–1013.

Wallenstein, S., and A. C. Fisher. 1977. The analysis of the two-period repeated
measurements crossover design with application to clinical trials. Biometrics
33:261–269.

Warton, D. I., R. A. Duursma, D. S. Falster, and S. Taskinen. 2012. smatr 3 – an R
package for estimation and inference about allometric lines. Methods in Ecology
and Evolution 3:257–259.

Appendix A: Derivation of the MAXN strategy

I thank Per Lundberg for providing the following derivation.

Assume that population growth in each i habitat follows the discrete Gompertz model:

$$N_{i(t+1)} = N_{i(t)}e^{r_i - b_i \ln N_{i(t)}} \tag{A1}$$

where N is population size at time t and $t + 1$, r is the intrinsic rate of population growth and b is the strength of density-dependence. Converting the equation to natural logarithms and rearranging terms yields the linear habitat fitness function:

$$\ln N_{i(t+1)} - \ln N_{i(t)} = r_i - b_i \ln N_{i(t)} \tag{A2}$$

where the left-hand term is a measure of fitness (W_i) which can be rewritten as:

$$W_i = e^{r_i} N_{i(t)}^{-b_i}. \tag{A3}$$

Taking the derivative,

$$\frac{dW}{dN} = -e^r bN^{-b-1}, \tag{A4}$$

setting it equal to zero, and accounting for the effects of relatedness, identifies the ESS in the zero-migration function set out by Morris et al. (2001) for habitats 1 and 2:

$$0 = e^{r_2}N_2^{-b_2} - e^{r_1}N_1^{-b_1} + R\left[N_2\left(-e^{r_2}N_2^{-b_2-1}\right) - N_1\left(-e^{r_1}N_1^{-b_1-1}\right)\right] \tag{A5}$$

where R is the coefficient of relatedness ($0 \leq R \geq 1$) of individuals, valued at 1 for clones. When individuals are unrelated ($R = 0$), a habitat selection strategy that equalizes mean individual fitness among habitats yields the ESS,

$$N_2 = e^{\frac{r_2 - r_1}{b_2}} N_1^{\frac{b_1}{b_2}}. \tag{A6}$$

However, when individuals are identically related ($R = 1$), the ESS maximizes inclusive

fitness (MAXN strategy):

$$N_2 = [e^{r_2}(1 - Rb_2)]^{\frac{1}{b_2}} [e^{r_1}N_1^{-b_1}(1 - Rb_1)]^{\frac{1}{-b_2}}. \tag{A7}$$

Appendix B: Experiment timeline

      I transferred all age-synchronized experimental populations into single homogeneous habitats (control, C) and two-habitat arenas (habitat selection, HS) after allowing 8 days for hatching and another 28 (youngest) to 34 (oldest) days for maturation (Day 42, Table B1). Control populations experienced no dispersal and habitat-selecting populations had opportunity to select habitat. Both treatments used the same five population sizes from a single synchronized culture. Four additional populations were included for the control group (with their designated homogeneous habitat in brackets, Table B1). I conducted experiments for each synchronized population (yielding 20 population sizes) at different times and completed them all within 164 days (Table B1).

Table B1. Timeline for tests of habitat selection and habitat-specific fitness for cloned populations of *Folsomia candida* (C = control, HS = habitat selection). Dates (YYYY-MM-DD) provided for events beginning with first establishment of the synchronized culture and followed by a homogeneous habitat or two-habitat arena treatment, two transfers among homogeneous habitats, the removal of adults, and finally a count of recruits.

Synchronized Culture	Population Sizes	Timeline				
		Dish Treatment (Day 42)	Transfer (Day 43)	Transfer (Day 52)	Remove (Day 61)	Count (Day 111)
SYNC A Initiated 2018-05-24	C & HS 40, 120, 440, 720, 800 C only 10 (12.5), 20 (25), 900 (37.5), 1000 (100)	2018-07-05	2018-07-06	2018-07-15	2018-07-24	2018-09-12
SYNC B Initiated 2018-06-15	C & HS 80, 200, 320, 520, 640 C only 10 (100), 20 (12.5), 900 (25), 1000 (37.5)	2018-07-27	2018-07-28	2018-08-06	2018-08-15	2018-10-04
SYNC C Initiated 2018-06-27	C & HS 240, 360, 480, 600, 760 C only 10 (37.5), 20 (100), 900 (12.5), 1000 (25)	2018-08-08	2018-08-09	2018-08-18	2018-08-27	2018-10-16
SYNC D Initiated 2018-07-15	C & HS 160, 280, 400, 560, 680 C only 10 (25), 20 (37.5), 900 (100), 1000 (12.5)	2018-08-26	2018-08-27	2018-09-05	2018-09-14	2018-11-03

Appendix C: Creating habitats

C1. Two types of petri dishes

I added substrate to petri dishes in order to create either a single homogeneous habitat used to estimate fitness, or two habitats in which I assessed habitat selection. For homogeneous habitats, I poured a 29.5 g slurry of plaster of Paris, activated charcoal, and distilled water into 100 x 15 mm VWR petri dishes (recipe = 156 g of plaster of Paris, 16.51 g of activated charcoal, and 156 mL of distilled water). I allowed the substrate to dry completely at room temperature in open dishes. I subtracted the tare (petri dish) weight from the total dry weight to determine the weight of dry substrate.

I created three sections in the two-habitat arenas by attaching a 50 x 9 mm BD Falcon petri dish lid in the centre of the large (100 mm) petri dishes, then created a waterproof barrier of all-purpose silicone caulking that divided the large dish in half (Fig. C1). All animals were released inside the Falcon lid. The area was slightly larger than that of the two habitats created by the silicone partition (21.2 cm^2 vs 18.4 cm^2 respectively). I excluded the habitat partition when calculating the area of each habitat. I poured just enough substrate mixture to reach the height of the lid of the inner small dish (recipe = 67.5 g of plaster of Paris, 7.16 g of activated charcoal, and 90 mL of distilled water).
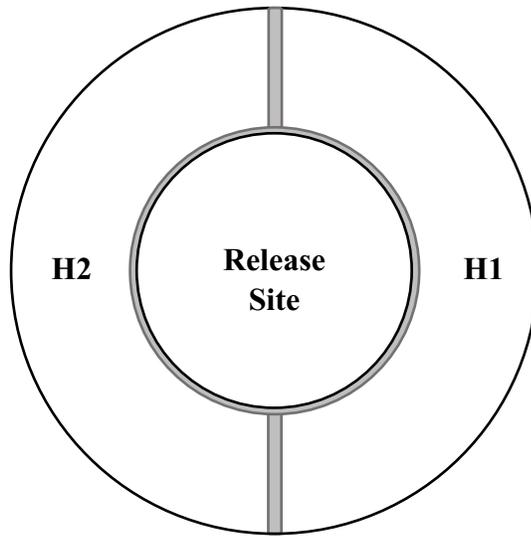
Figure C1. Top view of a two-habitat habitat arena. H2 and H1 indicate habitats 1 and 2, respectively. The inner dish constitutes the animal "release site". Grey colours indicate silicone caulking used to attach the release site and create the habitat partition.

C2. Substrate moisture concentrations

I created different substrate moisture concentrations with reference to best-fit linear versus quadratic regressions that I used to determine the relationship between dry substrate mass (g) and the volume of distilled water (mL) required for complete saturation (100%; determined by the volume of water that first produced a thin aqueous layer on the substrate surface).

Regression fits were exceptionally strong (Fig. C2). Saturation (S) in homogeneous habitat dishes was best predicted by a quadratic model (linear $R^2 = 0.96$ vs quadratic $R^2 = 0.97$; Fig. C2a):

$$S = 151.31965 - 14.91431(D) + 0.39246(D^2) \tag{C1}$$

where S is the volume of water in milliliters and D is the dry mass of substrate in grams. The parsimonious best-fit prediction for two-habitat dishes was linear (linear $R^2 = 0.97$ vs quadratic $R^2 = 0.97$; Fig. C2b):
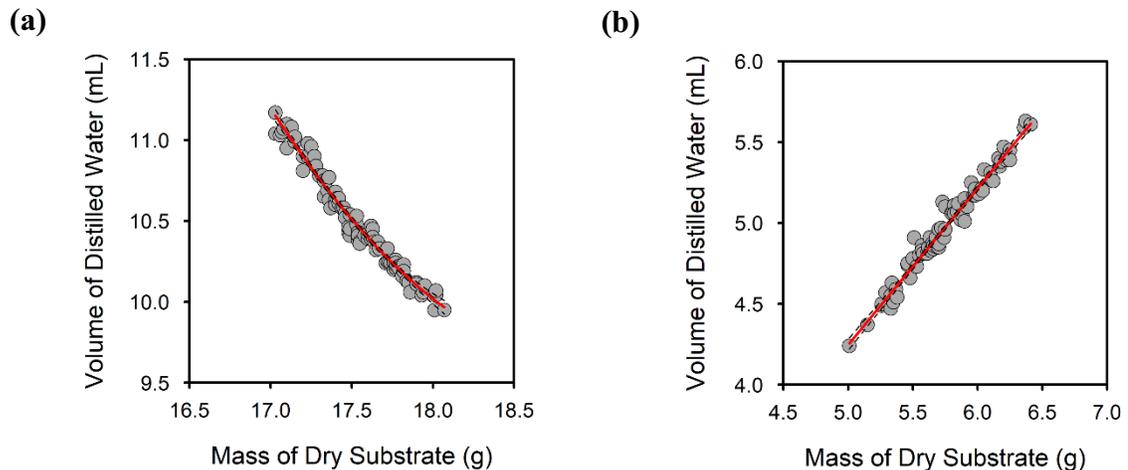
$$S = 0.96990(D) - 0.60382 \tag{C2}$$

Figure C2. Water volume required for complete saturation of dry substrate for: (a) control ($R^2 = 0.97$, $P < 0.001$), and (b) two-habitat petri dishes with a release site ($R^2 = 0.97$, $P < 0.001$).

C3. Habitat quality

I assessed the quality of different substrate moisture concentrations with 36 petri dishes comprised of 0 to 68.75% moisture at intervals of 6.25% (three dishes for each of 12 moisture concentrations). I placed three populations sizes ($N = 10$, 60, and 120) into each replicated petri dish and provided each with the same ratio of superabundant food (Table C1). Animals spent a 9-day quiescent period in each habitat before transfer to a second identical habitat for another 9 days of egg-laying, after which I recorded clutch formation and counted the number of dead animals. The two substrate moisture concentrations (0 and 6.25%) below 12.5% led to local extinctions; thus, I chose 12.5% (0% mortality, minimum egg production) as the low-quality habitat. I classified the 25% substrate moisture and 37.5% substrate moisture dishes as moderate quality (0% mortality with many small clutches; Table C1, Fig. C3).

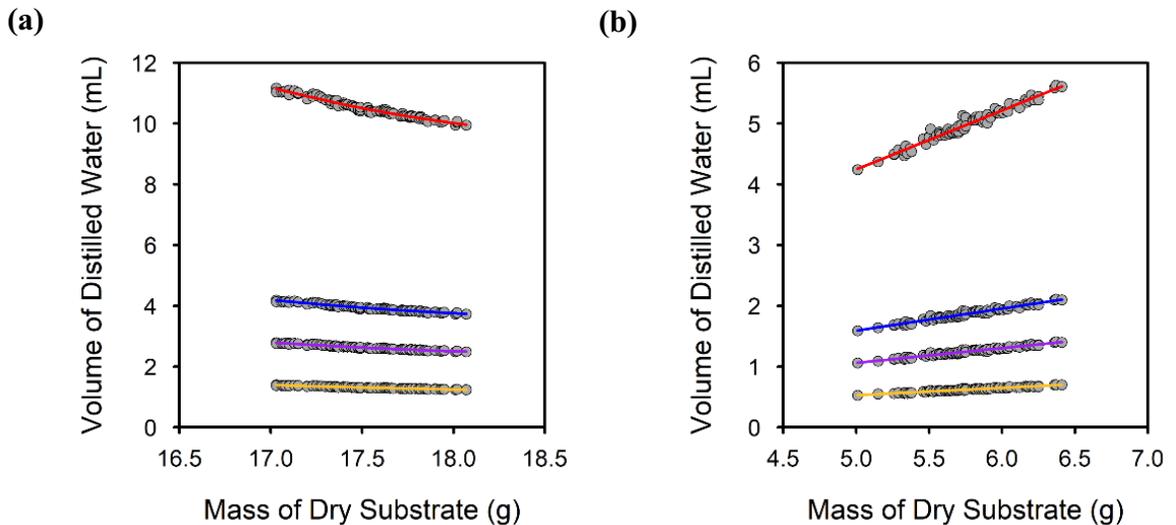**(a)**   **(b)**

Figure C3. Water volume for desired substrate moisture concentration as a function of dry substrate for: (a) controls and (b) two-habitat petri dishes. Coloured regressions correspond to substrate moisture concentrations: red = 100%, blue = 37.5%, purple = 25%, and gold = 12.5%.

Table C1. Egg-laying and adult survival of three different populations sizes living in habitats with different substrate moisture concentrations. Habitats chosen for experiments are highlighted: gold = 12.5 %, purple = 25 %, and blue = 37.5 %.

Habitat (% moisture)	N	Food pellets	Observations (mortality and egg-laying)
0	10	1	100% mortality, no eggs
0	60	6	100% mortality, no eggs
0	120	12	100% mortality, no eggs
6.25	10	1	100% mortality, no eggs
6.25	60	6	100% mortality, no eggs
6.25	120	12	100% mortality, no eggs
12.5	10	1	0% mortality, no eggs
12.5	60	6	0% mortality, no eggs
12.5	120	12	0% mortality, few eggs
18.75	10	1	0% mortality, no eggs
18.75	60	6	0% mortality, few scattered eggs
18.75	120	12	0% mortality, small clutch
25	10	1	0% mortality, some scattered eggs
25	60	6	0% mortality, small scattered clutches
25	120	12	0% mortality, small scattered clutches
31.25	10	1	0% mortality, some scattered eggs
31.25	60	6	0% mortality, small scattered clutches
31.25	120	12	0% mortality, small scattered clutches
37.5	10	1	0% mortality, some scattered eggs
37.5	60	6	0% mortality, some scattered eggs
37.5	120	12	0% mortality, small to medium scattered clutches
43.75	10	1	0% mortality, small egg clutch and scattered eggs
43.75	60	6	0% mortality, multiple small clutches
43.75	120	12	0% mortality, scattered small to medium clutches
50	10	1	0% mortality, large clutch
50	60	6	0% mortality, small scattered clutches
50	120	12	0% mortality, many small scattered clutches
56.25	10	1	0% mortality, many medium scattered clutches
56.25	60	6	0% mortality, small and medium scattered clutches
56.25	120	12	0% mortality, many medium scattered clutches
62.5	10	1	0% mortality, small scattered clutches
62.5	60	6	0% mortality, many small scattered clutches
62.5	120	12	0% mortality, many medium scattered clutches
68.75	10	1	0% mortality, many small scattered clutches
68.75	60	6	0% mortality, many medium scattered clutches
68.75	120	12	0% mortality, many small to medium clutches

C4. Conversion of abundance to standardized densities of habitat-selecting F. candida

I calculated densities (animals·cm^{-2}) of *F. candida* choosing high-quality (100%, periphery habitat plus the animal-release site) and low-quality habitats (all habitats with less than < 100% saturation). I multiplied these estimates by the full area of the petri dish (58 cm^2) and rounded them to the nearest integer in order to obtain an equivalent metric of density (animals 58·cm^{-2}) to that of animals moved to homogeneous dishes after habitat selection. Doing so allowed me to clearly indicate the actual number of animals used in each experiment.

C5. Renewal of moisture concentrations and resources

I sealed all dishes with parafilm (VWR Parafilm M, Catalogue #: 10014-058) to reduce potential changes in substrate moisture concentrations. Even so, I renewed moisture levels (using equations C1 and C2 respectively) weekly while also placing a new single yeast pellet in the centre of each dish before again re-sealing dishes with parafilm. Moisture levels remained stable and on average required addition of only 0.2 to 0.3 mL of distilled water each week.

Appendix D: Sensitivity of control fitness-density relationships

I tested the sensitivity of control fitness-density curves to their high-density tails by iterative least-squares regression on habitat fitness data with progressively fewer data points. I demonstrated the robustness of these fitness curves with successive estimates of parameter values following sequential elimination of the most extreme densities (11 points, Table D1).

Table D1. Iterated parameter values of control fitness-density relationships for each habitat (% moisture) following successive data point-deletion beginning at the highest density.

Data points	100% habitat		37.5% habitat		25% habitat		12.5% habitat	
	Intercept	Slope	Intercept	Slope	Intercept	Slope	Intercept	Slope
24	4.74	-0.81	5.26	-0.96	3.78	-0.72	3.90	-1.05
23	4.75	-0.82	5.21	-0.95	3.81	-0.72	3.96	-1.07
22	4.81	-0.83	5.26	-0.96	3.76	-0.71	3.60	-0.98
21	4.80	-0.83	5.23	-0.95	3.79	-0.72	3.81	-1.03
20	4.79	-0.82	5.14	-0.93	3.79	-0.72	3.59	-0.98
19	4.85	-0.84	5.14	-0.93	3.80	-0.72	3.53	-0.96
18	4.99	-0.87	5.24	-0.95	3.87	-0.74	3.63	-0.99
17	5.01	-0.88	5.25	-0.96	3.73	-0.70	3.64	-0.99
16	4.81	-0.83	5.14	-0.93	3.80	-0.72	3.57	-0.97
15	4.83	-0.83	5.18	-0.94	3.82	-0.72	3.71	-1.01
14	4.91	-0.85	5.14	-0.93	3.83	-0.73	3.82	-1.04
13	4.88	-0.84	5.13	-0.93	3.81	-0.72	3.85	-1.05
12	4.90	-0.84	5.13	-0.93	3.80	-0.72	4.02	-1.09
11	4.83	-0.83	5.08	-0.91	3.89	-0.75	4.14	-1.13

I then re-calculated expected isodars using the most extreme control fitness functions and found that only one case differed from the original habitat isodars (100% vs 37.5%; the MAXN strategy shifted towards empirical and IFD expectations, Fig. D1). Regardless of this convergence, the relative positions and slopes of the isodars were identical to those predicted from the full data set that I retained for subsequent analyses.
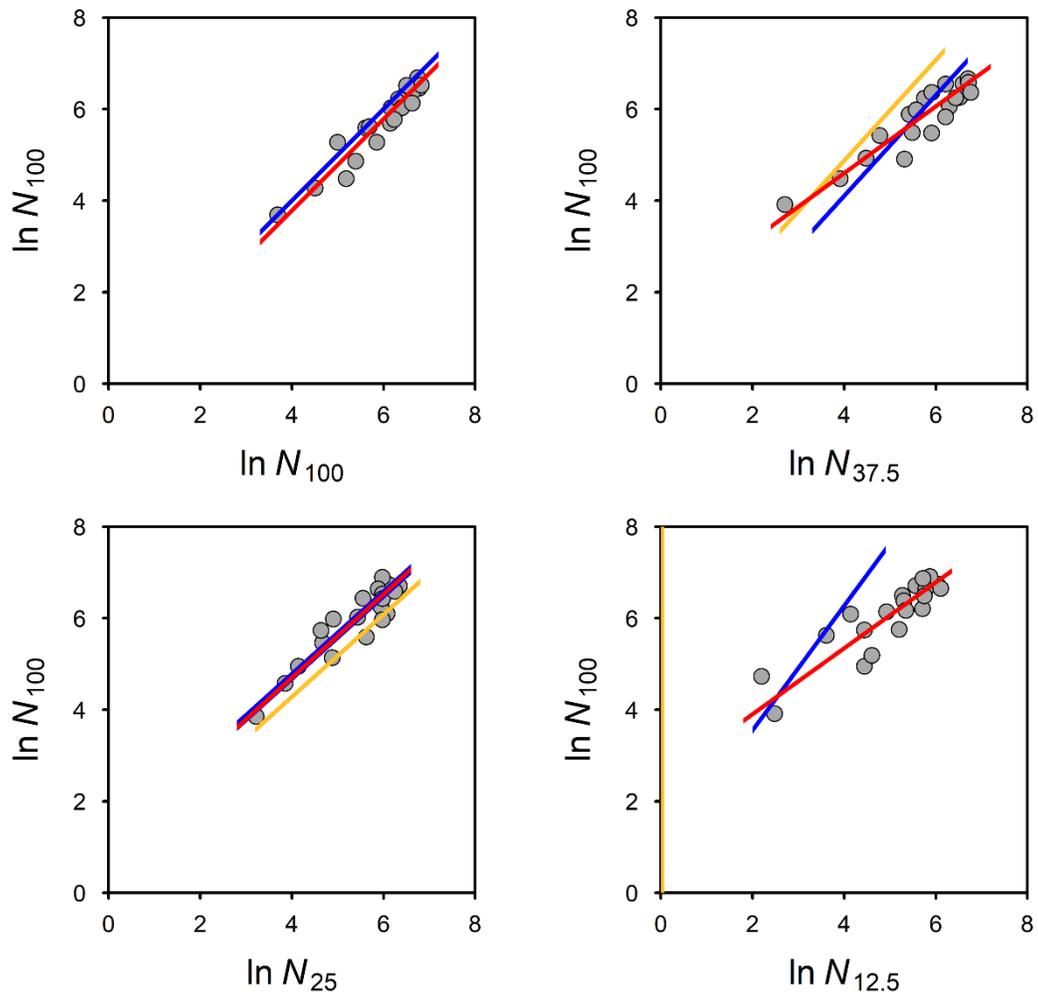

Figure D1. Empirical (red, shaded circles) and expected IFD (blue) and MAXN (gold) rarified isodars calculated from the most extreme control fitness functions (11 data points; compare with Fig. 3).